SDC

OPEN

# AGE-RELATED RETENTIONAL AVASCULAR PIGMENT EPITHELIAL DETACHMENT VIEWED WITH INDOCYANINE GREEN ANGIOGRAPHY

YONGYUE SU, MD,* XIONGZE ZHANG, MD, PHD,* LING CHEN, MD, PHD,† MIAOLING LI, MD, PHD,* YUHONG GAN, MD,* FENG WEN, MD, PHD*

**Purpose:** Age-related scattered hypofluorescent spots on late-phase indocyanine green angiography (ASHS-LIA) might represent hydrophobic neutral lipid deposits in the Bruch membrane. This study aimed to report retentional avascular pigment epithelial detachment (PED) associated with ASHS-LIA.

**Methods:** Patients aged ≥50 years who presented a single avascular serous PED without soft drusen or any other retinal or choroidal diseases were retrospectively included. Pigment epithelial detachment was classified as retentional, effusional, or mixed PED based on indocyanine green angiography. Multimodal images were qualitatively and quantitatively evaluated.

**Results:** This study included 74 eyes of 57 patients. Retentional PED, effusional PED, and mixed PED accounted for 91.9%, 4.1%, and 4.1%, respectively. All PEDs were located in the macular region. Seventeen (29.8%) included patients had bilateral PEDs and all were retentional PEDs with a high level of bilateral consistency in the characteristics of PED and ASHS-LIA. All retentional PEDs were within the bounds of ASHS-LIA. The area of retentional PED increased with the ASHS-LIA grade ($P = 0.030$).

**Conclusion:** Most age-related avascular serous PEDs are retentional PEDs. The location and area of retentional PEDs are consistent with the distribution of ASHS-LIA. These findings suggest that the hydrophobic neutral lipid deposits in the Bruch membrane might be involved in the pathogenesis and be a therapeutic target in age-related retentional avascular PED.

**RETINA** 42:1520–1528, 2022

Serous pigment epithelial detachment (PED) is defined as an abnormal accumulation of fluid under the retinal pigment epithelium (RPE).[1] In elderly patients, serous PED is frequently accompanied by choroidal neovascularization and may cause severe vision loss.[2] However, serous PED has been observed in the absence of choroidal neovascularization in elderly individuals.[1] The common cause for avascular serous PED could be central serous chorioretinopathy or idiopathic. The current treatment of avascular serous PED is limited because its classification and pathogenesis have not been fully revealed.[3–5]

Previous studies have speculated two possible mechanisms of the formation of avascular serous PED in elderly people. One is that an alteration in choroidal vascular permeability might cause the occurrence of serous PED, which is considered a variant of central serous chorioretinopathy.[6,7] This kind of PED manifests as PED with choroidal vascular hyperpermeability (CVH) on indocyanine green angiography (ICGA). Another potential mechanism is that lipid deposition in the Bruch membrane (BrM) with aging might form a hydrophobic barrier, resulting in the retention of fluid between the RPE and BrM.[5,8] However, in patients without drusen, there was no clinical evidence to support this speculation.[5,9]

In our previous studies, we reported a kind of specific hypofluorescent spots on late-phase ICGA called age-related scattered hypofluorescent spots on late-phase ICGA (ASHS-LIA), with no corresponding abnormalities detected by other multimodal imaging techniques.[10] ASHS-LIA is mainly located in the macular region, and can extend to the optic disk or even the whole posterior pole; the occurrence and grade of

ASHS-LIA increase with age.[10] According to its correlation with age, distribution, confluent feature, and relationship with soft drusen, ASHS-LIA might represent a correlate of subclinical diffuse lipid deposits in BrM: basal linear deposit (BLinD).[11] Basal linear deposit is a thin layer of neutral lipids consisting of the same membranous material as soft drusen but in a different form.[12] In our clinical observation, ASHS-LIA frequently appeared in eyes with avascular serous PED in elderly patients.

The purpose of this study was to describe the clinical features of avascular serous PED using multimodal imaging, to investigate the relationship between avascular serous PED and ASHS-LIA, and to classify the subtypes of age-related avascular serous PED.

## Methods

### *Patients*

This retrospective study was approved by the Institutional Review Board of Zhongshan Ophthalmic Center. All the research and data collection methods complied with the Declaration of Helsinki.

We reviewed the data of consecutive patients diagnosed with serous PED between October 2017 and October 2020 at Zhongshan Ophthalmic Center. The inclusion criteria were age ≥50 years and the presence of a single avascular serous PED in the study eye. Serous PED was diagnosed based on the following multimodal imaging manifestations: a yellowish-orange, circular or ovoid detachment of the RPE on color fundus photography (FP); intense early hyperfluorescence and progressive dye pooling on fundus fluorescein angiography (FFA); hypocyanescence or late dye pooling on ICGA; and a smooth, domed RPE elevation over an optically hyporeflective space on optical coherence tomography (OCT).[1]

The exclusion criteria were as follows: 1) evidence of choroidal neovascularization or polypoidal choroidal vasculopathy (PCV) on FFA, ICGA, OCT, or OCT angiography (OCTA) in the study eye; 2) soft drusen in either eye; 3) PED with RPE leakage sites or diffuse RPE atrophy, multiple small PEDs, or a history of central serous chorioretinopathy; 5) other concomitant diseases, such as inflammatory chorioretinal disease, choroidal tumors, glaucoma, or trauma; and 6) history of ophthalmologic intervention procedures performed on the study eye, such as laser coagulation, vitrectomy, antivascular endothelial growth factor injection, or photodynamic therapy.

### *Image Acquisition and Analysis*

All the included patients underwent a complete ophthalmic examination: best-corrected visual acuity examination, anterior segment examination, fundus biomicroscopy and multimodal imaging examinations, including FP (FF450 plus; Carl Zeiss, Germany or TRC-50X, Topcon, Japan), fundus autofluorescence, FFA, ICGA, infrared reflectance, OCT (Spectralis; Heidelberg Engineering, Heidelberg, Germany), and OCTA (RTVue 100; Optovue, Fremont, CA). The duration of ICGA for all study eyes was at least 30 minutes. OCT scans were performed on single high-definition vertical and horizontal lines across the center of the fovea with a 30° area. Forty-nine B-scans that covered an area of 30° × 25° centered on the fovea were also obtained for all eyes. The OCTA scanning area was captured in high-definition 6 mm × 6 mm sections centered on the fovea.

All the multimodal images were independently reviewed by two trained retinal specialists (Y.S. and X.Z). If the two retinal physicians held different opinions, discrepancies were referred to a third retinal specialist (F.W.) for final determination.

ASHS-LIA was defined as the presence of hypocyanescent spots on late-phase ICGA, clearly seen 30 minutes after dye injection.[10] ASHS-LIA showed a regular arrangement pattern with possible confluence and no corresponding abnormalities on color FP, fundus autofluorescence, FFA, and OCT. According to the affected region, ASHS-LIA was divided into three grades: Grade 1, macular region; Grade 2, macular region and region around the optic disk; and Grade 3, throughout the posterior pole.[10] Because ASHS-LIA has binocular symmetry,[13] we referred to late-phase ICGA images of both eyes to make a

From the *State Key Laboratory of Ophthalmology, Zhongshan Ophthalmic Center, Sun Yat-sen University, Guangdong Provincial Key Laboratory of Ophthalmology and Visual Science, Guangzhou, China; and †The First Affiliated Hospital of Chongqing Medical University, Chongqing Key Laboratory of Ophthalmology, and Chongqing Eye Institute, Chongqing, China.

Supported by the National Natural Science Foundation of China [grant number 81870674].

None of the authors has any conflicting interests to disclose.

Supplemental digital content is available for this article. Direct URL citations appear in the printed text and are provided in the HTML and PDF versions of this article on the journal's Web site (www.retinajournal.com).

Y. Su and X. Zhang contributed equally to this work.



Reprint requests: Feng Wen, MD, PhD, State Key Laboratory of Ophthalmology, Zhongshan Ophthalmic Center, Sun Yat-sen University, 54 South Xianlie Road, Guangzhou, China; e-mail: wenfeng208@foxmail.com

determination when the grading or the confluence of ASHS-LIA might be interfered by substantial PED in the macular region.

Choroidal vascular hyperpermeability was defined as round or irregular hypercyanescence with blurred contours that appeared approximately 5 minutes after indocyanine green injection.[14]

Three subtypes of included avascular serous PEDs, namely, retentional PED, effusional PED, and mixed PED, were differentiated according to different manifestations on ICGA. The names of the PED subtypes were derived from the key feature of a hypothesis investigated in this study about the mechanism underlying PED formation. Retentional PED was defined as serous PED surrounded by ASHS-LIA but without CVH. Effusional PED manifested as serous PED adjacent to or above CVH but without surrounding ASHS-LIA. Mixed PED was defined as serous PED with both surrounding ASHS-LIA and associated CVH.

The qualitative assessment included evaluation of the following characteristics: the presence and confluence of ASHS-LIA; the grade of ASHS-LIA and the presence of CVH; pachychoroidal features (dilated choroidal vessel lumen with a thinner inner choroidal layer on OCT within the area of CVH on ICGA) within or near the PED; and hyperpigmentation within the PED area and subretinal fluid (SRF) based on OCT. Hyperpigmentation was defined as clumps of gray or black pigment as seen in FP that corresponded to blocked fluorescence on dye angiography, and hyperreflective foci on the RPE with a shadow on OCT imaging.[15,16] The quantitative assessment included analysis of the subfoveal choroidal thickness (SFCT), the maximum PED height, and PED area. The SFCT and maximum PED height were measured on OCT using the Distance Measurement tool of the Spectralis system.[17] The PED area was determined by demarcating the borders of the PED on ICGA.

### *Statistical Analysis*

Statistical analysis was performed by using Statistical Package for the Social Sciences for Windows Ver. 25.0 (SPSS, Inc, Chicago, IL). One-way analysis of variance was performed to compare continuous variables among grades of ASHS-LIA. The chi-square test or Fisher exact test was used to compare categorical variables, when appropriate, among grades of ASHS-LIA. Trend analysis was used when multimodal imaging features showed a trend with the grade of ASHS-LIA. The paired-samples T-test, McNemar test, and the Wilcoxon signed-rank test were used to analyze differences between left and right eyes in patients with bilateral PED for continuous variables, categorical variables, and polytomous variables, respectively. Correlation and consistency were analyzed between left and right eyes in cases of bilateral involvement. $P$ values $<0.05$ were considered indicative of significance.

## Results

Seventy-four eyes of 57 Chinese patients with avascular serous PED were included in this study. The patient age ranged from 50 to 81 years, with a mean (±SD) age of 66.5 ± 7.0 years. Males accounted for 63.2% (36 patients). Among the 74 eyes with avascular serous PED, the mean best-corrected visual acuity was 0.29 ± 0.19 logMAR (Snellen equivalent: 20/39), and the mean (±SD) SFCT was 275.0 ± 81.4 $\mu$m. Of included eyes, retentional PED, effusional PED, and mixed PED accounted for 91.9% (68 of 74 eyes), 4.1% (3 of 74 eyes), and 4.1% (3 of 74 eyes), respectively. Figures 1 and 2 show representative multimodal images of retentional PED and effusional PED, respectively. All the included cases of PED were single PED located in the macular region.

### *Manifestations of Different Subtypes of Avascular Serous Pigment Epithelial Detachment*

The clinical features of different subtypes of avascular serous PED are shown in Table 1. The patients in the retentional PED group with an average age (±SD) of 66.9 ± 7.2 years were older than the patients in the effusional PED (64.3 ± 5.8 years) and mixed PED (63.0 ± 3.6 years) groups. Males accounted for 60.8%, 100.0%, and 60.7% of the patients in the retentional, effusional, and mixed PED groups, respectively. The mean PED area (±SD) was largest in the retentional PED (11.7 ± 7.7 mm$^2$) group, followed by the effusional PED (7.8 ± 6.6 mm$^2$) and mixed PED (6.1 ± 8.7 mm$^2$) groups. However, the mean SFCT (±SD) in the retentional PED group (273.6 ± 81.0 $\mu$m) was smaller than that in the effusional PED (291.7 ± 115.8 $\mu$m) and mixed PED (284.3 ± 87.4 $\mu$m) groups, and pachychoroidal features that were observed on OCT accounted for 0% (0 eyes), 100% (3 eyes), and 100.0% (3 eyes) of the eyes in the retentional, effusional, and mixed PED groups, respectively. The average maximum PED height was 473.9 ± 227.9, 517.7 ± 209.8, and 420.0 ± 463.7 $\mu$m in the retentional, effusional, and mixed PED groups, respectively. Hyperpigmentation within the PED area was present in 79.4%, 66.7%, and 33.3%, and SRF was present in 53.1%, 33.3%, and 33.3% in the retentional, effusional, and mixed PED groups, respectively.

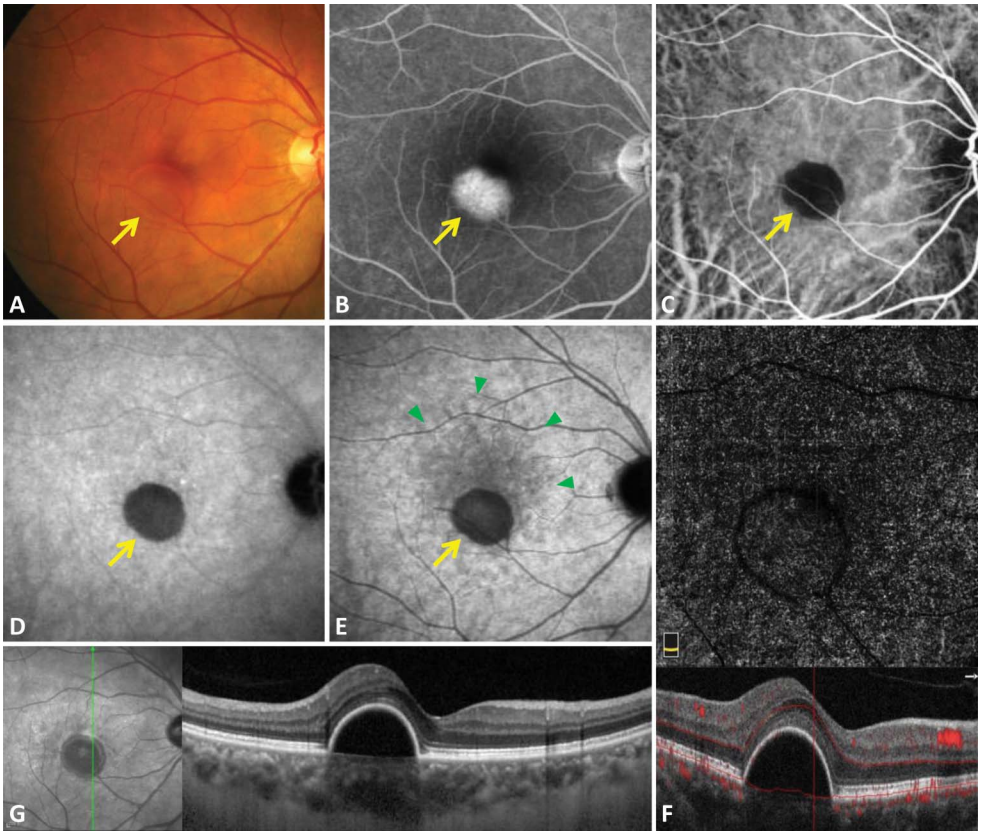


**Fig. 1.** Typical multimodal imaging of retentional PED. **A.** Color FP showed a yellowish-orange, dome-shaped elevation in the macular region (yellow arrow). **B–F.** Lack of CNV was confirmed by FFA, ICGA, and OCTA. **B.** Late-phase FFA showed dye pooling corresponding to PED (yellow arrow). **C–D.** Early-phase and mid-phase ICGA showed ovoid hypocyanescence corresponding to PED (yellow arrow) and absence of choroidal vascular hyperpermeability. **E.** Late-phase ICGA showed PED (yellow arrow) surrounded by partially confluent ASHS-LIA (green arrowhead) in the macular region. **G.** OCT showed hyporeflective space beneath the RPE corresponding to serous PED. No changes corresponding to ASHS-LIA were observed via color FP, FFA, OCTA, or OCT. CNV, choroidal neovascularization.

*Retentional Pigment Epithelial Detachment Eyes with Different Age-Related Scattered Hypofluorescent Spots on Late-Phase Indocyanine Green Angiography Grades*

In 68 eyes with retentional PED, ASHS-LIA could be divided into three grades according to the different regions affected (Figure 3). As Table 2 shows, the mean age significantly increased with the ASHS-LIA grade in patients with retentional PED, from 62.7 ± 6.6 to 68.7 ± 6.9 and 69.9 ± 6.3 years for Grades 1, 2, and 3, respectively ($P$ = 0.006; Grade 1 vs. Grade 2, $P$ = 0.007; Grade 1 vs. Grade 3, $P$ = 0.004; Grade 2 vs. Grade 3, $P$ = 0.607). All the retentional PED areas (100%) were within the bounds of ASHS-LIA. Confluent ASHS-LIA in the macula was detected in 56 out of 68 eyes (82.4%), of which 17 eyes (81.0%), 22 eyes (73.3%), and 17 eyes (100.0%) were found to have Grade 1, 2, and 3 ASHS-LIA, respectively ($P$ = 0.079). The mean area (±SD) of PED with Grade 1, 2, or 3 ASHS-LIA was 8.1 ± 5.9, 12.9 ± 8.2, and 14.1 ± 7.6 mm$^2$, respectively ($P$ = 0.030; Grade 1 vs. Grade 2, $P$ = 0.028; Grade 1 vs. Grade 3, $P$ = 0.016; Grade 2 vs. Grade 3, $P$ = 0.592), significantly increasing with the grade ($P$ for trend = 0.020). No significant difference was found among ASHS-LIA grades in sex, maximum PED height, SFCT, hyperpigmentation, or SRF.

*Retentional Pigment Epithelial Detachment With Bilateral Involvement*

Seventeen (29.8%) of the included patients had bilateral involvement, and all of them were in the retentional PED group. The characteristics of ASHS-LIA and retentional PED were similar in the right and left eyes (see **Figure 1**, **Supplemental Digital Content**, http://links.lww.com/IAE/B695). The bilateral grades of ASHS-LIA showed no difference ($P$ = 0.317), and high similarity was found in the left and right eyes (r = 0.904, $P < 0.001$). Macular ASHS-LIA confluence (15 patients, bilateral consistency = 88.2%) was bilaterally symmetrical. The average PED area in the right and left eyes in PED patients with bilateral involvement was 11.4 ± 7.2 and 12.9 ± 10.7 mm$^2$ ($P$ = 0.412), respectively, and a positive correlation was found in the PED area between the left and right eyes (r = 0.706, $P$ = 0.002). The average SFCT was 275.6 ± 90.2 and 258.6 ± 77.0 $\mu$m ($P$ = 0.222), respectively, and a positive correlation was found in the PED area between the left and right eyes (r = 0.837, $P < 0.001$). There was no difference in bilateral hyperpigmentation ($P$ = 1.000, bilateral consistency = 82.4%) and SRF ($P$ = 0.687, bilateral consistency = 64.7%) between the left and right eyes.

In addition, with the increase in ASHS-LIA grade from 1 to 2 in the retentional PED group, the proportion of patients with bilateral PED increased (22.2% in Grade 1% and 45.0% in Grade 2), but with the increase from Grade 2 to Grade 3 ASHS-LIA, this proportion decreased (30.9% in Grade 3; $P = 0.393$). The fellow eyes of patients with unilateral retentional PED exhibited PCV (32.0%), neovascular age-related macular degeneration (8.0%), hard drusen (44.0%), macular geographic atrophy (4.0%), and normal features (12.0%). The rates of PCV and neovascular age-related macular degeneration in the fellow eye increased with the ASHS-LIA grade, accounting for 18.2%, 55.6%, and 60.0% in Grades 1, 2, and 3, respectively ($P = 0.172$).

## Discussion

In this study, three subtypes of age-related avascular serous PED were differentiated according to ICGA manifestation: retentional PED, effusional PED, and mixed PED. More than nine out of 10 cases of avascular serous PED were classified as retentional PED associated with ASHS-LIA.

Serous PED can be defined as an abnormal accumulation of fluid under the RPE. Long-term detachment of the RPE in the macula may cause severe vision loss. Treatments for age-related avascular serous PED are not satisfactory because its pathogenesis has not yet been fully elucidated. The distinctive features of retentional and effusional PEDs indicate that the pathogenesis of age-related avascular serous PED varies by condition.

In this study, we found that a very large proportion of age-related avascular serous PED cases were classified as retentional PED. Moreover, the sites of retentional PED were all located in the macula and within the region of ASHS-LIA, and the retentional PED area increased with the size of the ASHS-LIA region. Macular ASHS-LIA in eyes with retentional PED was mostly confluent. These results imply that the incidence and extent of retentional PED are consistent with the density and distribution of ASHS-LIA. ASHS-LIA manifests as uniform hypocyanescence spots on late-phase ICGA.[18] Our recent studies have demonstrated that ASHS-LIA is age-related and bilaterally symmetrical, and might represent hydrophobic neutral lipid accumulation in BrM in the form of BLinD.[10,11,13] Basal linear deposit is a thin, tightly packed layer (0.4–2 $\mu$m) of lipoprotein deposits between the basal lamina of the RPE and the inner collagenous layer of BrM that forms during aging.[19–21] Previous pathology studies have also demonstrated that BLinD increases with age appeared to be more distributed in the macular region of the fundus than in the peripheral region,[22–25] similar to the location and the involved area of ASHS-LIA and retentional PED. These results suggest that BLinD, the candidate pathologic correlate for ASHS-LIA, might play a key role in the formation of age-related retentional PED.

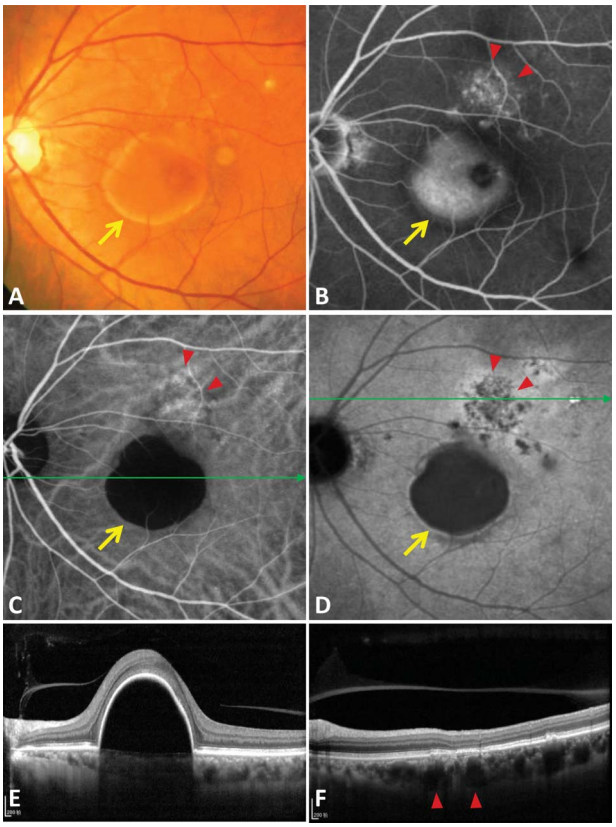


**Fig. 2.** Multimodal imaging of effusional PED. **A.** Color FP showed a yellowish-orange, dome-shaped elevation in the macular region (yellow arrow). **B.** Late-phase FFA showed dye pooling corresponding to PED (yellow arrow), with adjacent RPE window defect (red arrowhead). **C.** Early-phase ICGA showed choroidal vasodilation adjacent (red arrowhead) to PED hypocyanescence (yellow arrow) in the macular region. **D.** Late-phase ICGA showed PED hypocyanescence (yellow arrow) and hypocyanescence in the adjacent area (red arrowhead). **E.** OCT of the PED area (green line in C) showed empty space beneath the RPE. **F.** OCT of the hyperpermeability area (green line in D) showed dilated choroidal vessel lumen with a thinner inner choroidal layer (red arrowhead). Above the choroidal vessels, RPE atrophy corresponded to the hyperfluorescence of the RPE window defect on FFA.

Therefore, we hypothesized that the mechanism of retentional serous PED may be as follows (Figure 4): Under normal conditions, fluid flows in an overall vitreous-to-choroid direction across the BrM because of hydrostatic and osmotic forces.[26] With aging, the lipid deposits in BrM, especially BLinD, as a hydrophobic barrier might gradually cover the interfibrillar space of the inner collagenous layer of BrM, reducing the effective hydraulic conductivity of the BrM and partly blocking the normal, outward fluid efflux from

Table 1. Clinical Features of Different Subtypes of Avascular Serous PED

| | Retentional PED | Effusional PED | Mixed PED |
|---|---|---|---|
| No. of patients | 51 | 3 | 3 |
| Age, mean ± SD, years | 66.9 ± 7.2 | 64.3 ± 5.8 | 63.0 ± 3.6 |
| Sex, male, n (%) | 31 (60.8) | 3 (100.0) | 2 (66.7) |
| No. of eyes | 68 | 3 | 3 |
| PED in macula, n (%) | 68 (100.0) | 3 (100.0) | 3 (100.0) |
| CVH, n (%) | 0 (0.0) | 3 (100.0) | 3 (100.0) |
| ASHS-LIA, n (%) | 68 (100.0) | 0 (0.0) | 3 (100.0) |
| Maximum PED height, mean ± SD, $\mu$m | 473.9 ± 227.9 | 517.7 ± 209.8 | 420.0 ± 463.7 |
| PED area, mean ± SD, mm$^2$ | 11.7 ± 7.7 | 7.8 ± 6.6 | 6.1 ± 8.7 |
| SFCT, mean ± SD, $\mu$m | 273.6 ± 81.0 | 291.7 ± 115.8 | 284.3 ± 87.4 |
| Pachychoroidal feature | 0 (0.0) | 3 (100.0) | 3 (100.0) |
| Hyperpigmentation, n (%) | 54 (79.4) | 2 (66.7) | 1 (33.3) |
| SRF, n (%) | 34 (53.1) | 1 (33.3) | 1 (33.3) |

the RPE.[27–29] As the lipid deposits increase in BrM, especially that with confluence, the resistance of fluid passing through this lipid barrier at BrM exceeds the threshold of the equilibrium of fluid flow and ultimately leads to fluid retention between the basal lamina of the RPE and the inner collagenous layer of BrM (similar to a "barrier lake"), and in some cases, even mild SRF retention.[1,30,31] This retentional PED increases to a certain size that matches the grade of lipid barrier and then acts as a buffer pool for hydraulic resistance to form a new fluid flow equilibrium. However, it should be noted here that even with the presence of hydrophobic neutral lipid accumulation beneath a retentional PED, the interchange of material (especially the small molecules) and transport processes through the local BrM continues to some degree; thus, fluorescein could enter PED, causing dye accumulation on FFA.[1,29]

In addition, only retentional PED showed bilateral involvement, and the PED area in both eyes was consistent. This bilateral symmetry of retentional PED also supports the role of ASHS-LIA in its pathogenesis. In this study, as the ASHS-LIA increased from Grade 1 to Grade 2, the proportion of patients with bilateral retentional PED increased, but as the ASHS-LIA grade increased from Grade 2 to Grade 3, this proportion decreased. We also found that in eyes with unilateral retentional PED, the rate of PCV in the fellow eye gradually increased. ASHS-LIA might be involved in the pathogenesis of PCV.[13] Therefore, we considered that the decrease in the incidence of bilateral retentional PED from Grade 2 to Grade 3 ASHS-

Table 2. Clinical and Multimodal Imaging Features Among Different Grades of ASHS-LIA in Retentional PED Eyes

| | Grade 1 | Grade 2 | Grade 3 | *P* |
|---|---|---|---|---|
| No. of patients | 18 | 20 | 13 | |
| Age, mean ± SD, years | 62.7 ± 6.6 | 68.7 ± 6.9 | 69.9. ± 6.3 | **0.006*** |
| Sex, male, n (%) | 9 (50.0) | 12 (60.0) | 10 (76.9) | 0.316† |
| No. of eyes | 21 | 30 | 17 | |
| PED within the bounds of ASHS-LIA, n (%) | 21 (100.0) | 30 (100.0) | 17 (100.0) | NA |
| Confluent ASHS-LIA in macula, n (%) | 17 (81.0) | 22 (73.3) | 17 (100.0) | 0.079† |
| Maximum PED height, mean ± SD, $\mu$m | 456.0 ± 194.0 | 504.8 ± 268.4 | 437.6 ± 179.9 | 0.615* |
| PED area, mean ± SD, mm$^2$ | 8.1 ± 5.9 | 12.9 ± 8.2 | 14.1 ± 7.6 | **0.030*** |
| SFCT, mean ± SD, $\mu$m | 309.0 ± 70.6 | 249.3±64.6 | 287.4±101.1 | 0.071* |
| Hyperpigmentation, n (%) | 14 (66.7) | 26 (86.7) | 14 (82.4) | 0.208† |
| SRF, n (%) | 10 (50.0) | 13 (48.1) | 11 (64.7) | 0.532† |

*P* values in bold indicate $P < 0.05$.
*Analyzed using one-way ANOVA.
†Analyzed using the chi-square test or Fisher exact test.
ANOVA, analysis of variance.

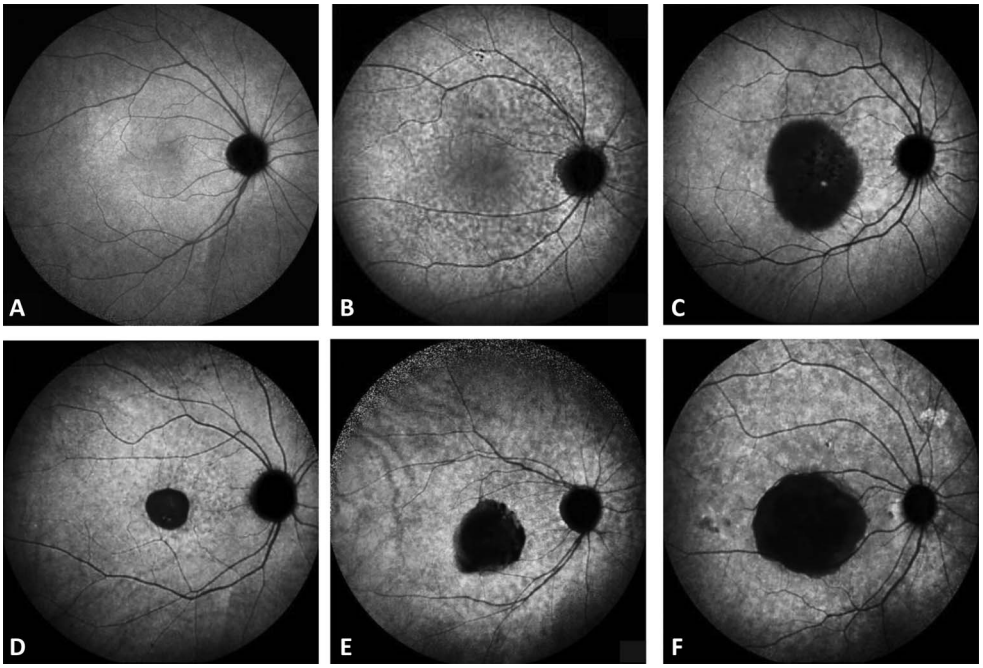


**Fig. 3.** ICGA characteristics of ASHS-LIA and gradation of ASHS-LIA in serous PED. **A.** Late-phase ICGA in an eye with a normal fundus. **B.** ASHS-LIA with macular confluence in an eye with a normal fundus. **C.** Retentional serous PED within ASHS-LIA of different grades. **D.** ASHS-LIA distributed in the macular region (Grade 1). (**E**) ASHS-LIA distributed in the macular region and the region around the optic disk (Grade 2). (**F**) ASHS-LIA distributed throughout the posterior pole, with partial confluence (Grade 3).

LIA may be due to the increase in PCV development in some eyes with Grade 3 ASHS-LIA eyes.

Three eyes showed an absence of ASHS-LIA but the presence of CVH, and were classified as having effusional PED. Effusional PED showed larger SFCT and dilated choroidal vessel lumen with a thinner inner choroidal layer. The multimodal features suggest that the mechanism of effusional PED might be different from that of retentional PED (Figure 4). Age-related effusional PED might be a variant of central serous chorioretinopathy or a sign of pachychoroid disease.[6] The increase in the choroidal vascular pressure reverses the flow of fluid to a choroid-to-retina direction, increasing the mechanical stress of the RPE. The fluid effuses from the choroid and passes through BrM, resulting in RPE elevation.[32] In addition, it should be noted that the effects of both CVH and ASHS-LIA on mixed PED are not contradictory. Choroidal compression and the lipid barrier on BrM could both exert effects, causing fluid accumulation.

The subtypes of age-related avascular serous PED are different not only morphologically but also in terms of the source of fluid accumulation, which might have a significant impact on current clinical practice. In retentional PED, the treatment might be similar to the oil spill strategy in age-related macular degeneration.[19] The effects of drugs such as statins and liver X receptor agonists or laser interventions are worthy of further exploration for confirmation.[33] However, antivascular endothelial growth factor therapy seems to be ineffective in the treatment of avascular serous PED.[3,4] In effusional PED, photodynamic therapy showed encouraging results.[6]

This study has several limitations. First, as a retrospective clinical study, selection bias is possible. The number of eyes with effusional PED and mixed PED in this study was limited because of their low proportions in elderly patients. However, the available data have indicated that there were differences in clinical characteristics among the different subtypes. Second, this study was limited by a lack of direct evidence of clinicopathologic correlation between ASHS-LIA and BLinD. Despite these limitations, our study substantively enriches our understanding of the pathogenesis of different types of age-related vascular serous PED, newly emphasizing the source of fluid accumulation in PED and providing directions for research into the treatment of these subtypes.

In conclusion, this study classified age-related avascular serous PED into three subtypes, namely, retentional, effusional, and mixed PED, according to ICGA manifestations. Nearly all cases of age-related avascular serous PED were classified as retentional PED within ASHS-LIA. Retentional PED was more frequently bilaterally involved, and its area increased with the ASHS-LIA grade. The results suggest that the hydrophobic neutral lipid deposits in BrM, shown as ASHS-LIA, might be involved in the pathogenesis and be a therapeutic target in retentional PED.

**Key words:** serous pigment epithelial detachment, age-related scattered hypofluorescent spots on late-phase indocyanine green angiography, basal linear deposit, lipid deposits, Bruch membrane, choroidal vascular hyperpermeability.

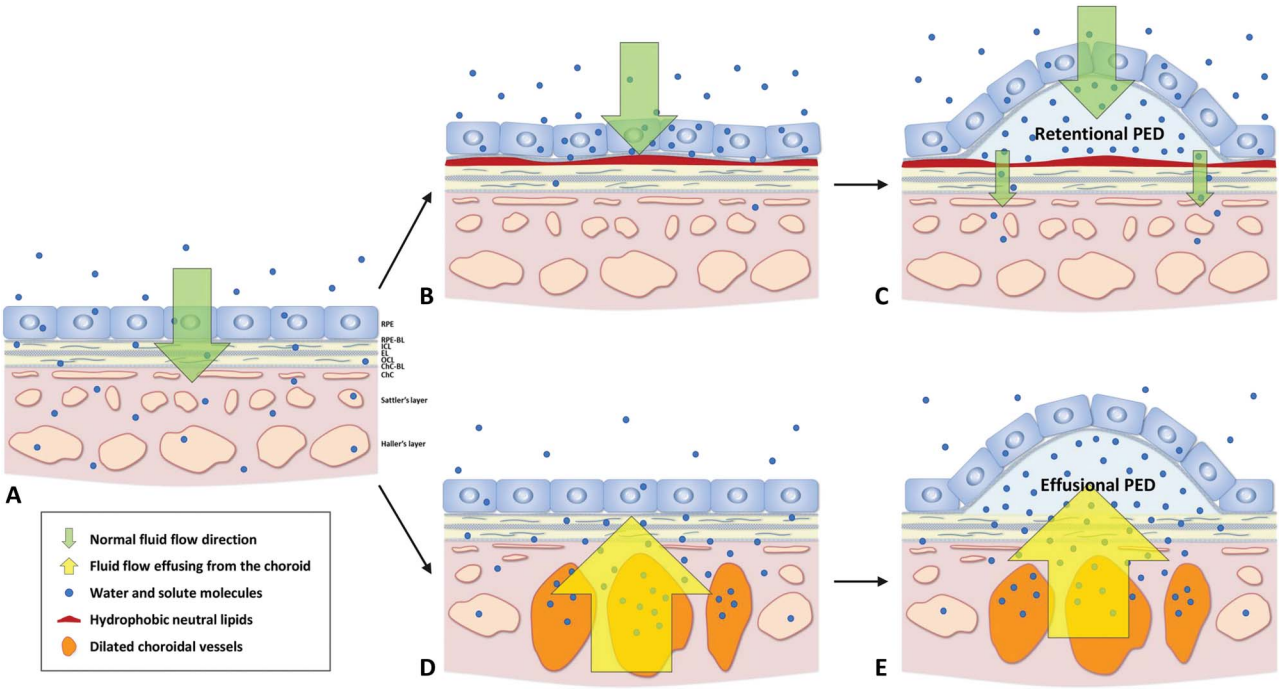


**Fig. 4.** Proposed pathophysiologic mechanism of retentional PED and effusional PED. **A.** Normal structure of the RPE, BrM, and choroid. The trilaminar BrM consists of the inner collagenous layer (ICL), elastic layer (EL), and outer collagenous layer (OCL). Under normal conditions, fluid flows (green arrow) in an overall vitreous-to-choroid direction because of the osmotic gradient. Between the RPE basal lamina (RPE-BL) and ICL of BrM (subRPE-BL space), hydrophobic neutral lipids accumulate in the form of BLinD with aging. The hydrophobic lipid barrier, especially with confluence, diminishes the membrane porosity and thus decreases the effective hydraulic conductivity of BrM (**B**). The resistance of the fluid flow at BrM exceeds the threshold level, eventually leading to fluid retention between the RPE-BL and the ICL of BrM. This retentional PED of a certain size that matches the grade of lipid barrier plays a role as buffer pool for hydraulic resistance and forms a new equilibrium of fluid flow (**C**). By contrast, in effusional PED, large choroidal vessels are dilated, and the above inner choroidal layers become thinned (**D**). An increase in choroidal vascular pressure generates reverse mechanical stress from the choroid to the RPE (yellow arrow from bottom to top). The fluid effuses from the choroid and passes through BrM, resulting in serous PED (**E**). ChC, choriocapillaris; ChC-BL, ChC basal lamina.

## References


1. Mrejen S, Sarraf D, Mukkamala SK, Freund KB. Multimodal imaging of pigment epithelial detachment: a guide to evaluation. Retina 2013;33:1735–1762.
2. Meredith TA, Braley RE, Aaberg TM. Natural history of serous detachments of the retinal pigment epithelium. Am J Ophthalmol 1979;88:643–651.
3. Ritter M, Bolz M, Sacu S, et al. Effect of intravitreal ranibizumab in avascular pigment epithelial detachment. Eye (Lond) 2010;24:962–968.
4. Tvenning AO, Hedels C, Krohn J, Austeng D. Treatment of large avascular retinal pigment epithelium detachments in age-related macular degeneration with aflibercept, photodynamic therapy, and triamcinolone acetonide. Clin Ophthalmol 2019; 13:233–241.
5. Bird AC. Doyne Lecture. Pathogenesis of retinal pigment epithelial detachment in the elderly; the relevance of Bruch's membrane change. Eye (Lond) 1991; 5 ( ): 1–12.
6. Kim KS, Lee WK. Photodynamic therapy with verteporfin for avascular serous pigment epithelial detachment in elderly Koreans. Retina 2010;30:93–99.
7. Giovannini A, Scassellati-Sforzolini B, D'Altobrando E, et al. Choroidal findings in the course of idiopathic serous pigment epithelium detachment detected by indocyanine green videoangiography. Retina 1997;17:286–293.
8. Pauleikhoff D, Löffert D, Spital G, et al. Pigment epithelial detachment in the elderly. Graefes Arch Clin Exp Ophthalmol 2002;240:533–538.
9. Curcio CA, Millican CL. Basal linear deposit and large drusen are specific for early age-related maculopathy. Arch Ophthalmol 1999;117:329–339.
10. Chen L, Zhang X, Liu B, et al. Age-related scattered hypofluorescent spots on late-phase indocyanine green angiography: the multimodal imaging and relevant factors. Clin Exp Ophthalmol 2018;46:908–915.
11. Chen L, Zhang X, Li M, et al. Drusen and age-related scattered hypofluorescent spots on late-phase indocyanine green angiography, a candidate correlate of lipid accumulation. Invest Ophthalmol Vis Sci 2018;59:5237–5245.
12. Curcio CA, Johnson M, Huang JD, Rudolf M. Apolipoprotein B-containing lipoproteins in retinal aging and age-related macular degeneration. J Lipid Res 2010;51:451–467.
13. Chen L, Zhang X, Li M, et al. Age-related scattered hypofluorescent spots on late-phase indocyanine green angiography as precursor lesions of polypoidal choroidal vasculopathy. Invest Ophthalmol Vis Sci 2019;60:2102–2109.
14. Spaide RF, Hall L, Haas A, et al. Indocyanine green videoangiography of older patients with central serous chorioretinopathy. Retina 1996;16:203–213.
15. Thiele S, Nadal J, Pfau M, et al. Prognostic value of retinal layers in comparison with other risk factors for conversion of

intermediate age-related macular degeneration. Ophthalmol Retina 2020;4:31–40.
16. Age-Related Eye Disease Study Research Group. The age-related eye disease study system for classifying age-related macular degeneration from stereoscopic color fundus photographs: the age-related eye disease study report number 6. Am J Ophthalmol 2001;132:668–681.
17. Koizumi H, Kano M, Yamamoto A, et al. Subfoveal choroidal thickness during aflibercept therapy for neovascular age-related macular degeneration: twelve-month results. Ophthalmology 2016;123:617–624.
18. Shiraki K, Moriwaki M, Kohno T, et al. Age-related scattered hypofluorescent spots on late-phase indocyanine green angiograms. Int Ophthalmol 1999;23:105–109.
19. Curcio CA, Johnson M, Rudolf M, Huang JD. The oil spill in ageing Bruch membrane. Br J Ophthalmol 2011;95:1638–1645.
20. Huang JD, Presley JB, Chimento MF, et al. Age-related changes in human macular Bruch's membrane as seen by quick-freeze/deep-etch. Exp Eye Res 2007;85:202–218.
21. Curcio CA. Soft drusen in age-related macular degeneration: biology and targeting via the oil spill strategies. Invest Ophthalmol Vis Sci 2018;59:D160–D181.
22. Curcio CA, Millican CL, Bailey T, Kruth HS. Accumulation of cholesterol with age in human Bruch's membrane. Invest Ophthalmol Vis Sci 2001;42:265–274.
23. Johnson M, Dabholkar A, Huang JD, et al. Comparison of morphology of human macular and peripheral Bruch's membrane in older eyes. Curr Eye Res 2007;32:791–799.
24. Haimovici R, Gantz DL, Rumelt S, et al. The lipid composition of drusen, Bruch's membrane, and sclera by hot stage polarizing light microscopy. Invest Ophthalmol Vis Sci 2001;42:1592–1599.
25. Holz FG, Sheraidah G, Pauleikhoff D, Bird AC. Analysis of lipid deposits extracted from human macular and peripheral Bruch's membrane. Arch Ophthalmol 1994;112:402–406.
26. Orr G, Goodnight R, Lean JS. Relative permeability of retina and retinal pigment epithelium to the diffusion of tritiated water from vitreous to choroid. Arch Ophthalmol 1986;104:1678–1680.
27. McCarty WJ, Chimento MF, Curcio CA, et al. Effects of particulates and lipids on the hydraulic conductivity of Matrigel. J Appl Physiol 2008;105:621–628.
28. Starita C, Hussain AA, Marshall J. Decreasing hydraulic conductivity of Bruch's membrane: relevance to photoreceptor survival and lipofuscinoses. Am J Med Genet 1995;57:235–237.
29. Starita C, Hussain AA, Pagliarini S, et al. Hydrodynamics of ageing Bruch's membrane: implications for macular disease. Exp Eye Res 1996;62:565–572.
30. Sheraidah G, Steinmetz R, Maguire J, et al. Correlation between lipids extracted from Bruch's membrane and age. Ophthalmology 1993;100:47–51.
31. Zayit-Soudry S, Moroz I, Loewenstein A. Retinal pigment epithelial detachment. Surv Ophthalmol 2007;52:227–243.
32. Daruich A, Matet A, Dirani A, et al. Central serous chorioretinopathy: recent findings and new physiopathology hypothesis. Prog Retin Eye Res 2015;48:82–118.
33. Guymer RH, Wu Z, Hodgson L, et al. Subthreshold nanosecond laser intervention in age-related macular degeneration: the LEAD randomized controlled clinical trial. Ophthalmology 2019;126:829–838.